

EM-Based Optimization Exploiting Partial Space Mapping and Exact Sensitivities

John W. Bandler, *Fellow, IEEE*, Ahmed S. Mohamed, *Student Member, IEEE*, Mohamed H. Bakr, *Member, IEEE*, Kaj Madsen, and Jacob Søndergaard

Abstract—We present a family of robust techniques for exploiting sensitivities in electromagnetic (EM)-based circuit optimization through space mapping (SM) technology. We utilize derivative information for parameter extractions and mapping updates. We exploit a partial SM (PSM) concept, where a reduced set of parameters is sufficient for parameter extraction optimization. It reflects the idea of tuning and execution time is reduced. Upfront gradients of both EM (fine) model and coarse surrogates can initialize possible mapping approximations. We introduce several effective approaches for updating the mapping during the optimization iterations. Examples include the classical Rosenbrock function, modified to illustrate the approach, a two-section transmission-line 10:1 impedance transformer and a microstrip bandstop filter with open stubs.

Index Terms—CAD, design automation, electromagnetic (EM) simulation, EM optimization, microwave filters, optimization methods, space mapping.

I. INTRODUCTION

USING an electromagnetic (EM) simulator (“fine” model) inside an optimization loop for the design process of microwave circuits can be prohibitive. Designers can overcome this problem by simplifying the circuit through circuit theory or by using the EM simulator with a coarser mesh. The space mapping (SM) approach [1], [2] relates a fine model to a physically based “coarse” surrogate. The fine model may be time intensive, field theoretic, and accurate, while the surrogate is a faster, circuit based, but less accurate, representation. SM introduces an efficient way to describe the relationship between the fine model and its surrogate. It makes effective use of the fast computation ability of the surrogate, on the one hand, and the accuracy of the fine model, on the other.

Surrogates in the context of filter design have been exemplified by Snel [3]. Practical benefits of empirical surrogates have also been demonstrated by Swanson and Wenzel [4]. They

Manuscript received March 26, 2002; revised August 13, 2002. This work was supported in part by the Natural Sciences and Engineering Research Council of Canada under Grant OGP0007239 and Grant STR234854-00, through the Micronet Network of Centres of Excellence and Bandler Corporation.

J. W. Bandler is with the Simulation Optimization Systems Research Laboratory, Department of Electrical and Computer Engineering, McMaster University, Hamilton, ON, Canada L8S 4K1 and also with the Bandler Corporation, Dundas, ON, Canada L9H 5E7 (e-mail: bandler@mcmaster.ca).

A. S. Mohamed is with the the Simulation Optimization Systems Research Laboratory, Department of Electrical and Computer Engineering, McMaster University, Hamilton, ON, Canada L8S 4K1.

M. H. Bakr is with the Department of Electrical and Computer Engineering, McMaster University, Hamilton, ON, Canada L8S 4K1.

K. Madsen and J. Søndergaard are with Informatics and Mathematical Modelling, Technical University of Denmark, DK-2800 Lyngby, Denmark.

Digital Object Identifier 10.1109/TMTT.2002.805188

achieved optimal mechanical adjustments by iterating between a finite element simulator and circuit simulator.

SM optimization involves the following steps. The “surrogate” is optimized to satisfy design specifications [5], thus providing the target response. A mapping is proposed between the parameter spaces of the fine model and its surrogate using a parameter extraction (PE) process. Then, an inverse mapping estimates the fine-model parameters corresponding to the (target) optimal surrogate parameters.

We present, for the first time, new techniques to exploit exact sensitivities in EM-based circuit design in the context of SM technology. If the EM simulator is capable of providing gradient information, these gradients can be exploited to enhance a coarse surrogate. New approaches for utilizing derivatives in the parameter extraction process and mapping update are presented.

We introduce also a new SM approach exploiting the concept of partial SM (PSM). Partial mappings were previously suggested in the context of neural space mapping [6]. Here, an efficient procedure exploiting a PSM concept is proposed. Several approaches for utilizing response sensitivities and PSM are suggested.

Exact sensitivities have been developed for nonlinear, harmonic-balance analyses [7], as well as implementable approximations such as the feasible adjoint sensitivity technique [8]. In the 1990s, Alessandri *et al.* spurred the application of the adjoint network method using a mode matching orientation [9]. Currently, we are developing the adjoint technique within a method of moments environment [10], [11]. These techniques facilitate powerful gradient-based optimizers. Our new work complements these efforts at gradient estimation for design optimization using EM simulations.

II. AGGRESSIVE SPACE MAPPING

A. Original Design Problem

The original design problem is

$$\mathbf{x}_f^* = \arg \min_{\mathbf{x}_f} U(\mathbf{r}_f(\mathbf{x}_f)). \quad (1)$$

Here, the fine-model response vector is denoted by $\mathbf{r}_f \in \mathbb{R}^{m \times 1}$, e.g., $|S_{11}|$ at selected frequency points, where m is the number of sample points. The fine-model point is denoted $\mathbf{x}_f \in \mathbb{R}^{n \times 1}$, where n is the number of design parameters. U is a suitable objective function. For example, U could be the minimax objective

function with upper and lower specifications. \mathbf{x}_f^* is the optimal design to be determined.

B. Parameter Extraction (PE)

PE is a crucial step in any SM algorithm. In PE, an optimization step is performed to extract a coarse-model point \mathbf{x}_c corresponding to the fine-model point \mathbf{x}_f that yields the best match between the fine model and its surrogate. The information stored in the design response \mathbf{r}_f may not be sufficient to describe the system under consideration properly. Thus, using only the design response in the PE may lead to nonuniqueness problems. Therefore, we need to obtain more information about the system and exploit it to extract the “best” coarse point and avoid nonuniqueness. For example, we may use responses such as real and imaginary parts of S parameters in the PE, even though we need only the magnitude of S_{11} to satisfy a certain design criterion. Now, we can assemble all the responses needed in the PE into one vector and define a new term, called a complete set of basic responses. The complete set of basic responses is designated by $\mathbf{R}(\mathbf{x}) \in \Re^{M \times 1}$, where $M = mN_r$, m is the number of simulation frequency points, and N_r is the number of basic responses. In this context, the fine and its surrogate (coarse) responses are denoted by \mathbf{R}_f and \mathbf{R}_c , respectively. The traditional PE is described by the optimization problem

$$\mathbf{x}_c^{(j)} = \arg \min_{\mathbf{x}_c} \left\| \mathbf{R}_f \left(\mathbf{x}_f^{(j)} \right) - \mathbf{R}_c \left(\mathbf{x}_c \right) \right\|. \quad (2)$$

C. Aggressive SM Approach

Aggressive SM solves the nonlinear system

$$\begin{aligned} \mathbf{f} &\triangleq \mathbf{P}(\mathbf{x}_f) - \mathbf{x}_c^* \\ &= \mathbf{x}_c - \mathbf{x}_c^* \\ &= \mathbf{0} \end{aligned} \quad (3)$$

for \mathbf{x}_f , where \mathbf{P} is a mapping defined between the two model spaces and $\mathbf{x}_c \in \Re^{n \times 1}$ is the corresponding point in the coarse space, $\mathbf{x}_c = \mathbf{P}(\mathbf{x}_f)$. First-order Taylor approximations are given by

$$\mathbf{P}(\mathbf{x}_f) \approx \mathbf{P} \left(\mathbf{x}_f^{(j)} \right) + \mathbf{J}_P \left(\mathbf{x}_f^{(j)} \right) \left(\mathbf{x}_f - \mathbf{x}_f^{(j)} \right). \quad (4)$$

This can be described as

$$\mathbf{x}_c \approx \mathbf{x}_c^{(j)} + \mathbf{J}_P \left(\mathbf{x}_f^{(j)} \right) \left(\mathbf{x}_f - \mathbf{x}_f^{(j)} \right) \Big|_{\text{Through PE}} \quad (5)$$

where the Jacobian of \mathbf{P} at the j th iteration is expressed by

$$\mathbf{J}_P \left(\mathbf{x}_f^{(j)} \right) = \left(\frac{\partial \mathbf{P}^T}{\partial \mathbf{x}_f} \right)^T \Big|_{\mathbf{x}_f=\mathbf{x}_f^{(j)}}. \quad (6)$$

Equation (5) illustrates the nonlinearity of the mapping, where $\mathbf{x}_c^{(j)}$ is related to $\mathbf{x}_f^{(j)}$ through the PE process which is a non-

linear optimization problem. Recalling (4) and (5), we state a useful definition of the mapping Jacobian at the j th iteration

$$\mathbf{J}_P^{(j)} \triangleq \left. \left(\frac{\partial \left(\mathbf{x}_c^{(j)T} \right)}{\partial \mathbf{x}_f} \right)^T \right|_{\text{PE}}. \quad (7)$$

We designate an approximation to this Jacobian by the square matrix $\mathbf{B} \in \Re^{n \times n}$, i.e., $\mathbf{B} \approx \mathbf{J}_P(\mathbf{x}_f)$.

From (3) and (5), we can formulate the system

$$\left(\mathbf{x}_c^{(j)} - \mathbf{x}_c^* \right) + \mathbf{B}^{(j)} \left(\mathbf{x}_f^{(j+1)} - \mathbf{x}_f^{(j)} \right) = \mathbf{0} \quad (8)$$

which can be rewritten in the useful form

$$\mathbf{B}^{(j)} \mathbf{h}^{(j)} = -\mathbf{f}^{(j)}. \quad (9)$$

Solving (9) for $\mathbf{h}^{(j)}$, the quasi-Newton step in the fine space provides the next tentative iterate $\mathbf{x}_f^{(j+1)}$

$$\mathbf{x}_f^{(j+1)} = \mathbf{x}_f^{(j)} + \mathbf{h}^{(j)}. \quad (10)$$

III. PROPOSED ALGORITHMS

A. PE Exploiting Sensitivity

We exploit the availability of the gradients of the fine model and surrogate responses to enhance the PE process. The Jacobian of the fine-model basic responses \mathbf{J}_f at \mathbf{x}_f and the corresponding Jacobian of the surrogate responses \mathbf{J}_c at \mathbf{x}_c can be obtained. Adjoint sensitivity analysis could be used to provide the exact derivatives, while finite differences are employed to estimate the derivatives if the exact derivatives are not available. Here, we present a new technique to formulate the PE to take into account not only the responses of the fine and its surrogate, but the corresponding gradients as well.

Through the traditional PE process, as in (2), we can obtain the point \mathbf{x}_c that corresponds to \mathbf{x}_f , such that

$$\mathbf{R}_f \approx \mathbf{R}_c. \quad (11)$$

Differentiating both sides of (11) with respect to \mathbf{x}_f , we obtain

$$\left(\frac{\partial \mathbf{R}_f^T}{\partial \mathbf{x}_f} \right)^T \approx \left(\frac{\partial \mathbf{R}_c^T}{\partial \mathbf{x}_c} \right)^T \left(\frac{\partial \mathbf{x}_c^T}{\partial \mathbf{x}_f} \right)^T. \quad (12)$$

Using (7), the relation (12) can be simplified to [12]

$$\mathbf{J}_f \approx \mathbf{J}_c \mathbf{B} \quad (13)$$

where \mathbf{J}_f and $\mathbf{J}_c \in \Re^{M \times n}$. Relation (13) assumes that \mathbf{J}_c is full rank and $M \geq n$, where M is the dimensionality of both \mathbf{R}_f and \mathbf{R}_c . Solving (13) for \mathbf{B} yields a least-squares solution [12]

$$\mathbf{B} = (\mathbf{J}_c^T \mathbf{J}_c)^{-1} \mathbf{J}_c^T \mathbf{J}_f. \quad (14)$$

At the j th iteration we obtain $\mathbf{x}_c^{(j)}$ through a gradient parameter extraction (GPE) process. In GPE, we match not only the

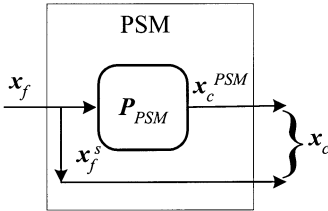


Fig. 1. Partial space mapping (PSM).

responses, but also the derivatives of both models through the optimization problem

$$\mathbf{x}_c^{(j)} = \arg \min_{\mathbf{x}_c} \left\| \begin{bmatrix} \mathbf{e}_0^T & \lambda \mathbf{e}_1^T & \cdots & \lambda \mathbf{e}_n^T \end{bmatrix}^T \right\|, \quad \lambda \geq 0 \quad (15)$$

where λ is a weighting factor, $\mathbf{E} = [\mathbf{e}_1 \mathbf{e}_2 \dots \mathbf{e}_n]$, and

$$\begin{aligned} \mathbf{e}_0 &= \mathbf{R}_f(\mathbf{x}_f^{(j)}) - \mathbf{R}_c(\mathbf{x}_c) \\ \mathbf{E} &= \mathbf{J}_f(\mathbf{x}_f^{(j)}) - \mathbf{J}_c(\mathbf{x}_c) \mathbf{B}. \end{aligned} \quad (16)$$

The nonuniqueness in the PE may lead to divergence or oscillatory behavior. Exploiting available gradient information enhances the uniqueness of the PE process. It also reflects the idea of multipoint extraction (MPE) [13], [14] in which simultaneous matching of a number of points of both spaces takes place.

B. PSM

Utilizing a reduced set of the physical parameters of the coarse space might be sufficient to obtain an adequate surrogate for the fine model. A selected set of the design parameters are mapped onto the coarse space, and the rest of them ($\mathbf{x}_f^s \subset \mathbf{x}_f$) are directly passed. The mapped coarse parameters are denoted by $\mathbf{x}_c^{\text{PSM}} \in \mathbb{R}^{k \times 1}$, $k \leq n$, where n is the number of design parameters. PSM is illustrated in Fig. 1. It can be represented in the matrix form by

$$\mathbf{x}_c = \begin{bmatrix} \mathbf{x}_c^{\text{PSM}} \\ \mathbf{x}_f^s \end{bmatrix} = \begin{bmatrix} \mathbf{P}_{\text{PSM}}(\mathbf{x}_f) \\ \mathbf{x}_f^s \end{bmatrix}. \quad (17)$$

In this context, (13) becomes

$$\mathbf{J}_f \approx \mathbf{J}_c^{\text{PSM}} \mathbf{B}^{\text{PSM}} \quad (18)$$

where $\mathbf{B}^{\text{PSM}} \in \mathbb{R}^{k \times n}$ and $\mathbf{J}_c^{\text{PSM}} \in \mathbb{R}^{M \times k}$ is the Jacobian of the coarse model at $\mathbf{x}_c^{\text{PSM}}$. Solving (18) for \mathbf{B}^{PSM} yields the least-squares solution at the j th iteration

$$\mathbf{B}^{\text{PSM}(j)} = \left(\mathbf{J}_c^{\text{PSM}(j)T} \mathbf{J}_c^{\text{PSM}(j)} \right)^{-1} \mathbf{J}_c^{\text{PSM}(j)T} \mathbf{J}_f^{(j)}. \quad (19)$$

Relation (9) becomes underdetermined since \mathbf{B}^{PSM} is a fat rectangular matrix, i.e., the number of columns is greater than the number of rows. The minimum norm solution for $\mathbf{h}^{(j)}$ is given by

$$\mathbf{h}_{\text{min norm}}^{(j)} = \mathbf{B}^{\text{PSM}(j)T} \left(\mathbf{B}^{\text{PSM}(j)} \mathbf{B}^{\text{PSM}(j)T} \right)^{-1} \left(-\mathbf{f}^{(j)} \right). \quad (20)$$

The coarse-model parameters $\mathbf{x}_c^{\text{PSM}}$ used in the PE can be determined by the sensitivity analysis proposed by Bandler *et al.*

[15]. It chooses the parameters that the coarse-model response is sensitive to.

C. Mapping Update Alternatives

If we have exact derivatives of both the fine and coarse model, we can use them to obtain \mathbf{B} at each iteration using a least-squares solution as in (14). Note that this matrix can be iteratively fed back into the GPE process and refined before making a step in the fine-model space. We can also use (19) to update \mathbf{B}^{PSM} .

If we do not have exact derivatives, various approaches to initializing or constraining \mathbf{B} and \mathbf{B}^{PSM} can be devised; for example, we can use finite differences (perturbations). Either matrix may be updated using a Broyden update [16]. Hybrid schemes can be formally developed following the integrated gradient approximation approach to optimization by Bandler *et al.* [17]. One hybrid approach incorporates the use of perturbations and Broyden formula. Utilizing this approach reduces the effort of calculating exact derivatives. Perturbations are used to obtain an initial good approximation to \mathbf{B} and \mathbf{B}^{PSM} at the starting point. Then, the Broyden formula is used to update both matrices in the subsequent iterations.

On the assumption that the fine and coarse models share the same physical background, Bakr *et al.* [18] suggested that \mathbf{B} could be better conditioned, in the PE process, if it is constrained to be close to the identity matrix \mathbf{I} by

$$\mathbf{B} = \arg \min_{\mathbf{B}} \left\| \left[\mathbf{e}_1^T \cdots \mathbf{e}_n^T \eta \Delta \mathbf{b}_1^T \cdots \eta \Delta \mathbf{b}_n^T \right]^T \right\|_2^2 \quad (21)$$

where η is a weighting factor and \mathbf{e}_i and $\Delta \mathbf{b}_i$ are the i th columns of \mathbf{E} and $\Delta \mathbf{B}$, respectively, defined as

$$\begin{aligned} \mathbf{E} &= \mathbf{J}_f - \mathbf{J}_c \mathbf{B} \\ \Delta \mathbf{B} &= \mathbf{B} - \mathbf{I}. \end{aligned} \quad (22)$$

The analytical solution of (21) is given by

$$\mathbf{B} = (\mathbf{J}_c^T \mathbf{J}_c + \eta^2 \mathbf{I})^{-1} (\mathbf{J}_c^T \mathbf{J}_f + \eta^2 \mathbf{I}). \quad (23)$$

D. Proposed Algorithms

Algorithm 1 Full Mapping/GPE/Jacobian update

Step 1 Set $j = 1$. Initialize $\mathbf{B} = \mathbf{I}$ for the PE process. Obtain the optimal coarse-model design \mathbf{x}_c^* and use it as the initial fine-model point

$$\mathbf{x}_f^{(1)} = \mathbf{x}_c^* = \arg \min_{\mathbf{x}_c} U(\mathbf{r}_c(\mathbf{x}_c)). \quad (24)$$

Comment Minimax optimization is used to obtain the optimal coarse solution.

Step 2 Execute a preliminary GPE step as in (15).

Comment Match the responses and the corresponding gradients.

Step 3 Refine the mapping matrix \mathbf{B} using Jacobians (14).

Comment A least-squares solution is used to refine a square matrix \mathbf{B} using Jacobians.

Step 4 Stop if

$$\left\| \mathbf{f}^{(j)} \right\| \leq \varepsilon_1 \text{ or } \left\| \mathbf{R}_f^{(j)} - \mathbf{R}_c^* \right\| \leq \varepsilon_2. \quad (25)$$

Comment Loop until the stopping conditions are satisfied.

Step 5 Solve (9) for $\mathbf{h}^{(j)}$.

Step 6 Find the next $\mathbf{x}_f^{(j+1)}$ using (10).

Step 7 Perform GPE as in (15).

Step 8 Update $\mathbf{B}^{(j)}$ using (14).

Comment A least-squares solution is used to update \mathbf{B} at each iteration exploiting Jacobians.

Step 9 Set $j = j + 1$ and go to Step 4.

Algorithm 2 Partial SM/GPE/Jacobian update

Step 1 Set $j = 1$. Initialize $\mathbf{B}^{\text{PSM}} = [\mathbf{I}^{\text{PSM}} \mathbf{0}]$ for the PE process. Obtain the optimal coarse-model design \mathbf{x}_c^* and use it as the initial fine-model point as in (24).

Step 2 Execute a preliminary GPE step as in (15).

Step 3 Refine the mapping matrix \mathbf{B}^{PSM} using (19).

Comment A least-squares solution is used to refine a rectangular matrix \mathbf{B}^{PSM} using Jacobians.

Step 4 Stop if (25) holds.

Comment Loop until the stopping conditions are satisfied.

Step 5 Evaluate $\mathbf{h}^{(j)}$ using (20).

Comment A minimum norm solution for a quasi-Newton step $\mathbf{h}^{(j)}$ in the fine space is used.

Step 6 Find the next $\mathbf{x}_f^{(j+1)}$ using (10).

Step 7 Perform GPE as in (15).

Step 8 Use (19) to update $\mathbf{B}^{\text{PSM}(j)}$.

Comment A least-squares solution is used to update \mathbf{B}^{PSM} at each iteration.

Step 9 Set $j = j + 1$ and go to Step 4.

Algorithm 3 Partial SM/PE/Hybrid approach for mapping update

Step 1 Set $j = 1$. Initialize $\mathbf{B}^{\text{PSM}} = [\mathbf{I}^{\text{PSM}} \mathbf{0}]$ for the PE process. Obtain the optimal coarse-model design \mathbf{x}_c^* and use it as the initial fine-model point as in (24).

Step 2 Execute a preliminary traditional PE step as in (2).

Step 3 Refine the mapping matrix \mathbf{B}^{PSM} using (19).

Comment A least-squares solution is used to refine a rectangular matrix \mathbf{B}^{PSM} using Jacobians.

Step 4 Stop if (25) holds.

Comment Loop until the stopping conditions are satisfied.

Step 5 Evaluate $\mathbf{h}^{(j)}$ using (20).

Step 6 Find the next $\mathbf{x}_f^{(j+1)}$ using (10).

Step 7 Perform traditional PE as in (2).

Step 8 Update $\mathbf{B}^{\text{PSM}(j)}$ using a Broyden formula.

Comment A hybrid approach is used to update \mathbf{B}^{PSM} .

Step 9 Set $j = j + 1$ and go to Step 4.

The output of the algorithms is the fine space mapped optimal design $\bar{\mathbf{x}}_f$ and the mapping matrix \mathbf{B} (Algorithm 1) or \mathbf{B}^{PSM} (Algorithms 2 and 3).

IV. EXAMPLES

A. Rosenbrock Banana Problem [12], [19]

Test problems based on the classical Rosenbrock banana function are studied. We let the original Rosenbrock function

$$R_c = 100(x_2 - x_1^2)^2 + (1 - x_1)^2 \quad (26)$$

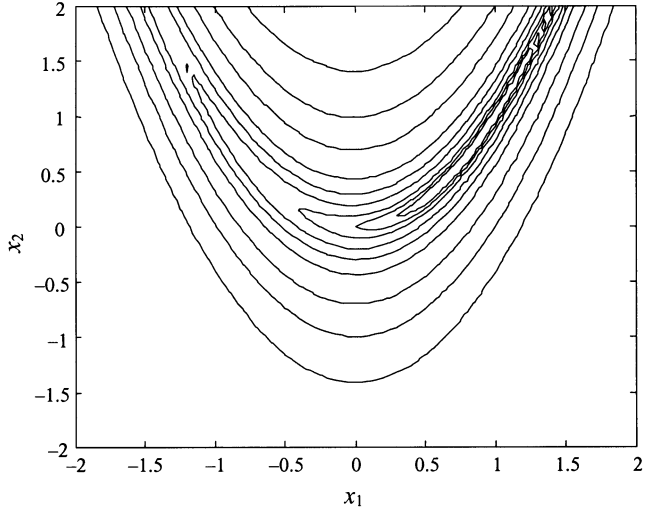


Fig. 2. Contour plot of the “coarse” original Rosenbrock banana function.

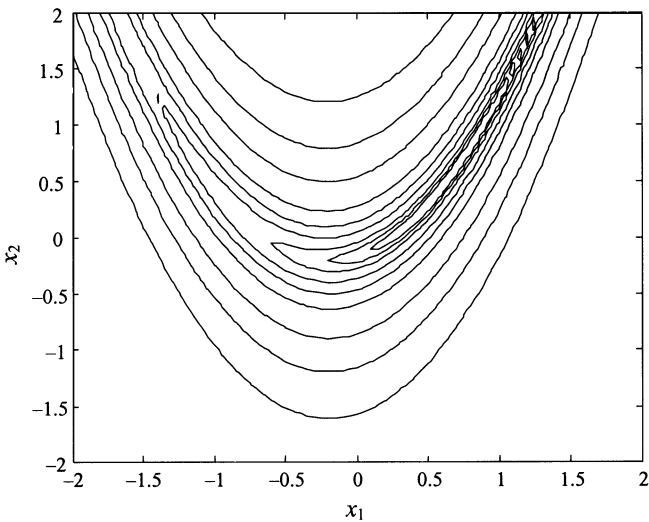


Fig. 3. Contour plot of the “fine” shifted Rosenbrock banana function.

be a “coarse” model. The optimal solution is $\mathbf{x}_c^* = [1.0 \ 1.0]^T$. A contour plot is shown in Fig. 2.

Case 1: Shifted Rosenbrock Problem: We propose a “fine” model as a shifted Rosenbrock function

$$R_f = 100((x_2 + \alpha_2) - (x_1 + \alpha_1)^2)^2 + (1 - (x_1 + \alpha_1))^2 \quad (27)$$

where

$$\boldsymbol{\alpha} = \begin{bmatrix} \alpha_1 \\ \alpha_2 \end{bmatrix} = \begin{bmatrix} -0.2 \\ 0.2 \end{bmatrix}. \quad (28)$$

The optimal fine-model solution is $\mathbf{x}_f^* = \mathbf{x}_c^* - \boldsymbol{\alpha} = [1.2 \ 0.8]^T$ (see Fig. 3 for a contour plot).

We apply Algorithm 1. Exact “Jacobians” \mathbf{J}_f and \mathbf{J}_c are used in the GPE process and in mapping update. The algorithm converges in one iteration to the exact solution (see Table I).

Case 2: Transformed Rosenbrock Problem: A “fine” model is described by the transformed Rosenbrock function

$$R_f = 100(u_2 - u_1^2)^2 + (1 - u_1)^2 \quad (29)$$

TABLE I
“SHIFTED” ROSENROCK BANANA PROBLEM

Iteration	$\mathbf{x}_c^{(j)}$	$\mathbf{f}^{(j)}$	$\mathbf{B}^{(j)}$	$\mathbf{h}^{(j)}$	$\mathbf{x}_f^{(j)}$	$R_f^{(j)}$
0	$\begin{bmatrix} 1.0 \\ 1.0 \end{bmatrix}$	---	---	---	$\begin{bmatrix} 1.0 \\ 1.0 \end{bmatrix}$	31.4
1	$\begin{bmatrix} 0.8 \\ 1.2 \end{bmatrix}$	$\begin{bmatrix} -0.2 \\ 0.2 \end{bmatrix}$	$\begin{bmatrix} 1.0 & 0.0 \\ 0.0 & 1.0 \end{bmatrix}$	$\begin{bmatrix} 0.2 \\ -0.2 \end{bmatrix}$	$\begin{bmatrix} 1.2 \\ 0.8 \end{bmatrix}$	0
	$\begin{bmatrix} 1.0 \\ 1.0 \end{bmatrix}$	$\begin{bmatrix} 0 \\ 0 \end{bmatrix}$				

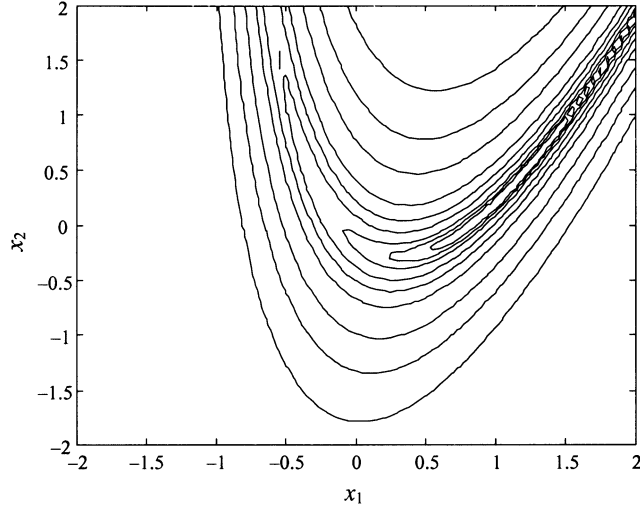


Fig. 4. Contour plot of the “fine” transformed Rosenbrock banana function.

where

$$\mathbf{u} = \begin{bmatrix} 1.1 & -0.2 \\ 0.2 & 0.9 \end{bmatrix} \mathbf{x} + \begin{bmatrix} -0.3 \\ 0.3 \end{bmatrix}. \quad (30)$$

The exact solution evaluated by the inverse transformation is $\mathbf{x}_f^* = [1.2718447 \ 0.4851456]^T$ to seven decimals. A contour plot is shown in Fig. 4. Applying Algorithm 1, we get a solution, to a very high accuracy, in six iterations (see Table II for details).

B. Capacitively Loaded 10:1 Impedance Transformer [20]

We apply Algorithm 2 to a two-section transmission line (TL) 10:1 impedance transformer. We consider a “coarse” model as an ideal two-section TL, where the “fine” model is a capacitively loaded TL with capacitors $C_1 = C_2 = C_3 = 10 \text{ pF}$. The fine and coarse models are shown in Figs. 5 and 6, respectively. Design parameters are normalized lengths L_1 and L_2 , with respect to the quarter-wave length L_q at the center frequency 1 GHz, and characteristic impedances Z_1 and Z_2 . Normalization makes the problem well posed. Thus, $\mathbf{x}_f = [L_1 \ L_2 \ Z_1 \ Z_2]^T$. Design specifications are

$$|S_{11}| \leq 0.5, \quad \text{for } 0.5 \text{ GHz} \leq \omega \leq 1.5 \text{ GHz}$$

with 11 points per frequency sweep. We utilize the real and imaginary parts of S_{11} in the GPE (15). The fine and surrogate responses can be easily computed as a function of the design parameters using circuit theory [21]. We solve (15) using the

TABLE II
“TRANSFORMED” ROSENROCK BANANA PROBLEM

Iteration	$\mathbf{x}_c^{(j)}$	$\mathbf{f}^{(j)}$	$\mathbf{B}^{(j)}$	$\mathbf{h}^{(j)}$	$\mathbf{x}_f^{(j)}$	$R_f^{(j)}$
0	$\begin{bmatrix} 1.0 \\ 1.0 \end{bmatrix}$	---	---	---	$\begin{bmatrix} 1.0 \\ 1.0 \end{bmatrix}$	108.3
1	$\begin{bmatrix} 0.526 \\ 1.384 \end{bmatrix}$	$\begin{bmatrix} -0.474 \\ 0.384 \end{bmatrix}$	$\begin{bmatrix} 1.01 & -0.05 \\ 0.01 & 1.01 \end{bmatrix}$	$\begin{bmatrix} 0.447 \\ -0.385 \end{bmatrix}$	$\begin{bmatrix} 1.447 \\ 0.615 \end{bmatrix}$	5.119
2	$\begin{bmatrix} 1.185 \\ 1.178 \end{bmatrix}$	$\begin{bmatrix} 0.185 \\ 0.178 \end{bmatrix}$	$\begin{bmatrix} 0.96 & -0.13 \\ -0.096 & 1.06 \end{bmatrix}$	$\begin{bmatrix} -0.218 \\ -0.187 \end{bmatrix}$	$\begin{bmatrix} 1.23 \\ 0.427 \end{bmatrix}$	4.4E-3
3	$\begin{bmatrix} 0.967 \\ 0.929 \end{bmatrix}$	$\begin{bmatrix} -0.033 \\ -0.071 \end{bmatrix}$	$\begin{bmatrix} 1.09 & -0.19 \\ 0.168 & 0.92 \end{bmatrix}$	$\begin{bmatrix} 0.0429 \\ 0.0697 \end{bmatrix}$	$\begin{bmatrix} 1.273 \\ 0.497 \end{bmatrix}$	1.8E-6
4	$\begin{bmatrix} 1.001 \\ 1.001 \end{bmatrix}$	$\begin{bmatrix} 0.001 \\ 0.001 \end{bmatrix}$	$\begin{bmatrix} 1.10001 & -0.1999 \\ 0.1999 & 0.9001 \end{bmatrix}$	$\begin{bmatrix} -0.001 \\ -0.002 \end{bmatrix}$	$\begin{bmatrix} 1.2719 \\ 0.4952 \end{bmatrix}$	5E-10
5	$\begin{bmatrix} 1.00002 \\ 1.00004 \end{bmatrix}$	$\begin{bmatrix} 0.2E-4 \\ 0.4E-4 \end{bmatrix}$	$\begin{bmatrix} 1.1 & -0.2 \\ 0.2 & 0.9 \end{bmatrix}$	$\begin{bmatrix} 0.3E-4 \\ 0.5E-4 \end{bmatrix}$	$\begin{bmatrix} 1.2718 \\ 0.4951 \end{bmatrix}$	3E-17
6	$\begin{bmatrix} 1.0 \\ 1.0 \end{bmatrix}$	$\begin{bmatrix} 0.1E-8 \\ 0.3E-8 \end{bmatrix}$	$\begin{bmatrix} 1.1 & -0.2 \\ 0.2 & 0.9 \end{bmatrix}$	$\begin{bmatrix} 0.2E-8 \\ 0.5E-8 \end{bmatrix}$	$\begin{bmatrix} x_f^* \\ x_f^* \end{bmatrix}$	9E-29

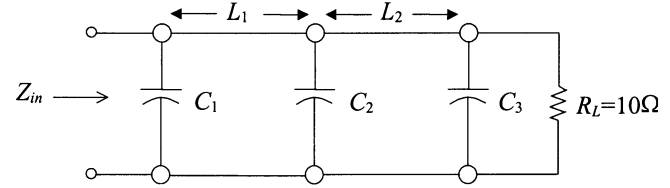


Fig. 5. Two-section impedance transformer: “fine” model.

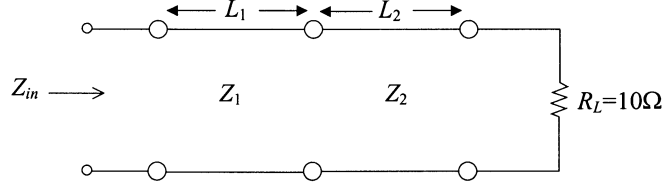


Fig. 6. Two-section impedance transformer: “coarse” model.

TABLE III
COARSE MODEL SENSITIVITIES WITH RESPECT TO THE DESIGN PARAMETERS FOR THE CAPACITIVELY LOADED IMPEDANCE TRANSFORMER

Parameter	\hat{S}_i
L_1	0.98
L_2	1.00
Z_1	0.048
Z_2	0.048

Levenberg–Marquardt algorithm for nonlinear least-squares optimization available in the Matlab Optimization Toolbox [22].

Case 1: Based on a sensitivity analysis [15] for the design parameters of the coarse model shown in Table III we note that the normalized lengths $[L_1 \ L_2]$ are the key parameters. Thus, we consider $\mathbf{x}_c^{\text{PSM}} = [L_1 \ L_2]^T$, while $\mathbf{x}_f^s = [Z_1 \ Z_2]^T$ are kept fixed at the optimal values, i.e., $Z_1 = 2.23615 \Omega$ and $Z_2 = 4.47230 \Omega$. We employ adjoint sensitivity-analysis techniques [23] to obtain the exact Jacobians of the fine and coarse models. We initialize \mathbf{B}^{PSM} by using the Jacobian information of both models at the starting point as in (19). The algorithm converges in a single iteration (two fine-model evaluations). The corresponding responses are illustrated in Figs. 7 and 8, respec-

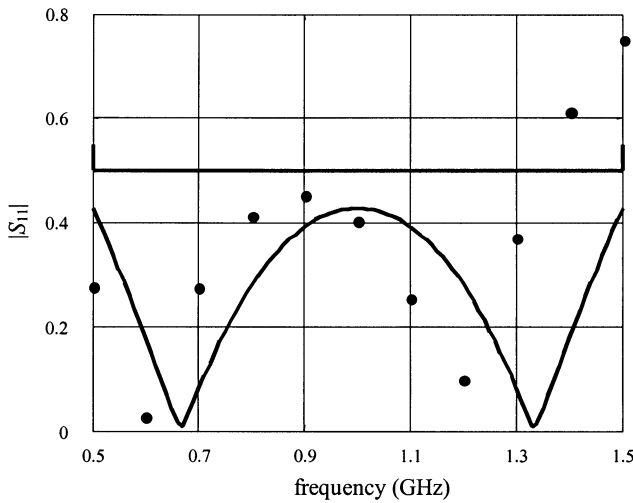


Fig. 7. Optimal coarse-model target response (—) and the fine-model response at the starting point (●) for the capacitively loaded 10:1 transformer with L_1 and L_2 as the PSM coarse-model parameters.

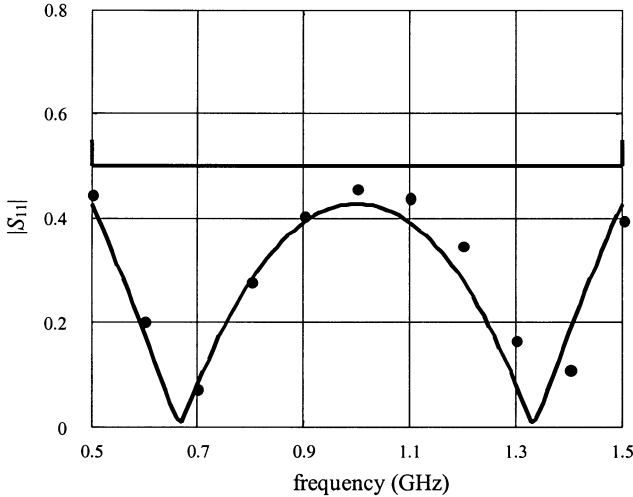


Fig. 8. Optimal coarse-model target response (—) and the fine-model response at the final design (●) for the capacitively loaded 10:1 transformer with L_1 and L_2 as the PSM coarse-model parameters.

tively. The final mapping is

$$\mathbf{B}^{\text{PSM}} = \begin{bmatrix} 1.075 & 0.087 & 0.006 & 0.002 \\ 0.049 & 1.139 & -0.008 & 0.006 \end{bmatrix}.$$

This result confirms the sensitivity analysis presented in Table III. It supports our decision of taking into account only $[L_1 \ L_2]$, represented by the first and the second columns in \mathbf{B}^{PSM} , as design parameters. As is well known, the effect of the capacitance in the fine model can only be substantially compensated by a change of the length of a TL. Therefore, changes of $[Z_1 \ Z_2]$ hardly affect the final response.

The reduction of $\|\mathbf{x}_c - \mathbf{x}_c^*\|_2$ versus iteration is shown in Fig. 9. The reduction of the objective function U in Fig. 10 also illustrates convergence (two iterations).

Case 2: We apply Algorithm 2 for $\mathbf{x}_c^{\text{PSM}} = [L_1]$. The result is similar to Fig. 8. Convergence is in a single iteration (two

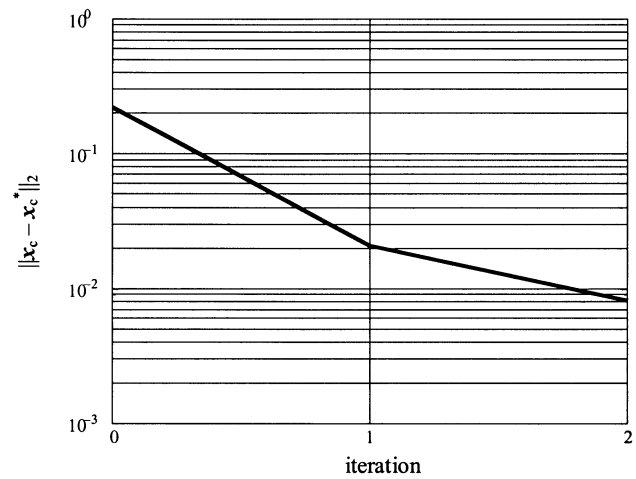


Fig. 9. $\|\mathbf{x}_c - \mathbf{x}_c^*\|_2$ versus iteration for the capacitively loaded 10:1 transformer with L_1 and L_2 as the PSM coarse-model parameters.

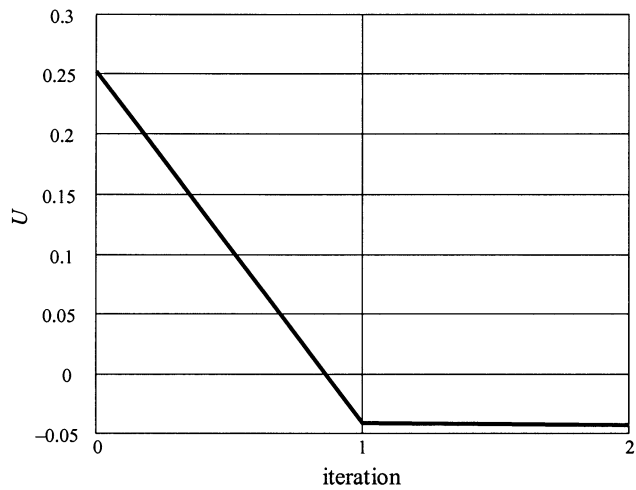


Fig. 10. U versus iteration for the capacitively loaded 10:1 transformer with L_1 and L_2 as the PSM coarse-model parameters.

fine-model evaluations). The final mapping is

$$\mathbf{B}^{\text{PSM}} = [1.371 \ 0.909 \ 0.0033 \ 0.0055].$$

As we can see, changes in $[L_1]$ represented by the first element in \mathbf{B}^{PSM} are significant. However, the second parameter $[L_2]$ is affected also. This arises from the fact that $[L_1 \ L_2]$ have the same physical effect; namely, that of length in a TL.

Case 3: We apply Algorithm 2 for $\mathbf{x}_c^{\text{PSM}} = [L_2]$. The result is similar to Fig. 8 and it converges in a single iteration (two fine-model evaluations). The final mapping is

$$\mathbf{B}^{\text{PSM}} = [0.8989 \ 1.186 \ -0.0043 \ 0.0087].$$

As in case 2, changes in one parameter, $[L_2]$ in this case, have a dominant role. This affects $[L_1]$, the parameter which shares the same physical nature.

The initial and final designs for all three cases are shown in Table IV. We realize that the algorithm aims to rescale the TL lengths to match the responses in the PE process (see Fig. 7). In

TABLE IV
INITIAL AND FINAL DESIGNS FOR THE CAPACITIVELY LOADED
IMPEDANCE TRANSFORMER

Parameter	$\mathbf{x}_f^{(0)}$ (L_1 and L_2)	$\mathbf{x}_f^{(1)}$ (L_1)	$\mathbf{x}_f^{(1)}$ (L_2)
L_1	1.0	0.8995	0.8631
L_2	1.0	0.8228	0.9126
Z_1	2.23615	2.2369	2.2352
Z_2	4.47230	4.4708	4.4716
L_1 and L_2 are normalized lengths			
Z_1 and Z_2 are in ohm			

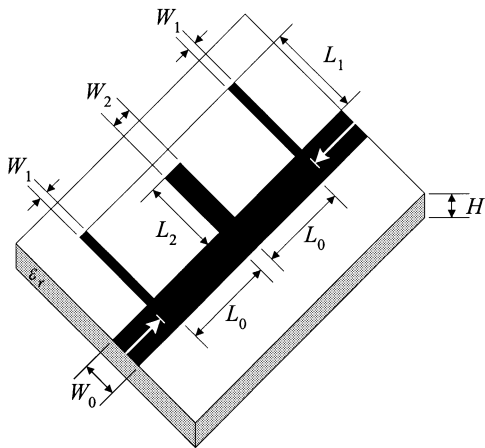


Fig. 11. Bandstop microstrip filter with open stubs: "fine" model.

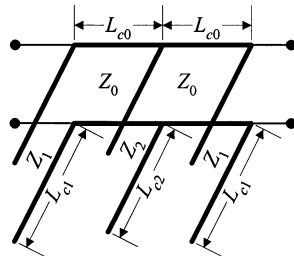


Fig. 12. Bandstop microstrip filter with open stubs: "coarse" model.

all cases, both $[L_1 \ L_2]$ are reduced by similar overall amounts, as expected.

By carefully choosing a reduced set of design parameters, we can affect other "redundant" parameters and the overall circuit response as well, which implies the idea of tuning. Nevertheless, the use of the entire set of design parameters should give the best result.

C. Bandstop Microstrip Filter With Open Stubs [6]

Algorithm 3 is applied to a symmetrical bandstop microstrip filter with three open stubs. The open-stub lengths are L_1 , L_2 , L_1 and the corresponding stub widths are W_1 , W_2 , W_1 . An alumina substrate with thickness $H = 25$ mil, width $W_0 = 25$ mil, dielectric constant $\epsilon_r = 9.4$, and loss tangent = 0.001

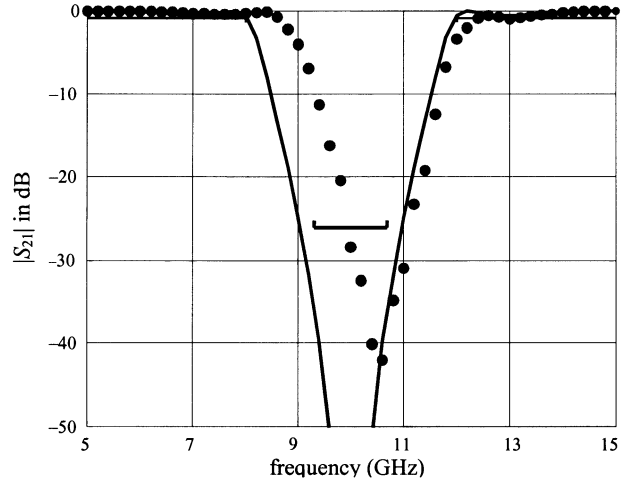


Fig. 13. Optimal OSA90/hope coarse target response (—) and *em* fine-model response at the starting point (●) for the bandstop microstrip filter using a fine frequency sweep (51 points) with L_1 and L_2 as the PSM coarse-model parameters.

TABLE V
COARSE-MODEL SENSITIVITIES WITH RESPECT TO DESIGN PARAMETERS
FOR THE BANDSTOP MICROSTRIP FILTER

Parameter	\hat{S}_i
W_1	0.065
W_2	0.077
L_0	0.677
L_1	1.000
L_2	0.873

is used for a 50- Ω feeding line. The design parameters are $\mathbf{x}_f = [W_1 \ W_2 \ L_0 \ L_1 \ L_2]^T$. The design specifications are

$$\begin{aligned} |S_{21}| &\leq 0.05 \text{ for } 9.3 \text{ GHz} \leq \omega \leq 10.7 \text{ GHz} \\ |S_{21}| &\geq 0.9 \text{ for } 12 \text{ GHz} \leq \omega \leq 8 \text{ GHz}. \end{aligned}$$

Sonnet's *em* [24] driven by Empipe [25] is employed as the fine model, using a high-resolution grid with a 1 mil \times 1 mil cell size. As a coarse model, we use simple TLs for modeling each microstrip section and classical formulas [21] to calculate the characteristic impedance and the effective dielectric constant of each TL. It is seen that $L_{c2} = L_2 + W_0/2$, $L_{c1} = L_1 + W_0/2$, and $L_{c0} = L_0 + W_1/2 + W_2/2$. We use OSA90/hope [25] built-in TL elements TRL. The fine model and its surrogate coarse model are illustrated in Figs. 11 and 12, respectively.

Using OSA90/hope, we can get the optimal coarse solution at 10 GHz as $\mathbf{x}_c^* = [4.560 \ 9.351 \ 107.80 \ 111.03 \ 108.75]^T$ (in mils). We use 21 points per frequency sweep. The coarse- and fine-model responses at the optimal coarse solution are shown in Fig. 13 (fine sweep is used only for illustration). We utilize the real and imaginary parts of S_{11} and S_{21} in the traditional PE. Sensitivity analysis for the coarse model is given in Table V. During the PE, we consider $\mathbf{x}_c^{\text{PSM}} = [L_1 \ L_2]^T$ while $\mathbf{x}_f^s = [W_1 \ W_2 \ L_0]^T$ are held fixed at the optimal coarse solution. Finite differences estimate the fine and coarse

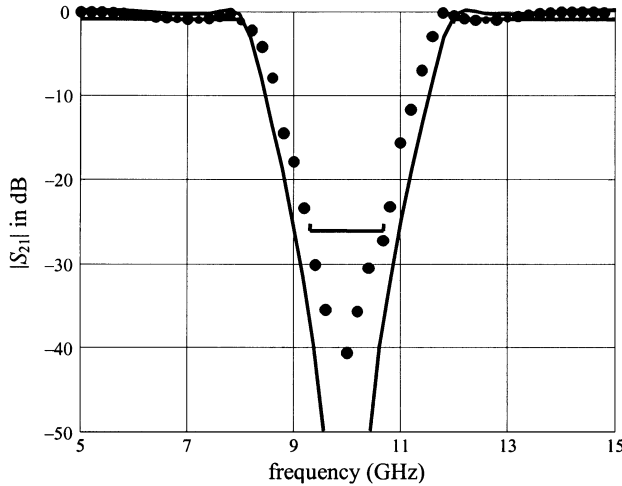


Fig. 14. Optimal OSA90/hope coarse target response (—) and *em* fine-model response at the final design (●) for the bandstop microstrip filter using a fine frequency sweep (51 points) with L_1 and L_2 as the PSM coarse-model parameters.

Jacobians used to initialize B^{PSM} , as in (19). A hybrid approach is used to update B^{PSM} at each iteration.

Algorithm 3 converges in five iterations. The PE execution time for the whole process is 59 min on an IBM-IntelliStation¹ machine. The optimal coarse-model response and the final design fine response are depicted in Fig. 14. The convergence of the algorithm is depicted in Fig. 15, where the reduction of $\|\mathbf{x}_c - \mathbf{x}_c^*\|_2$ versus iteration is illustrated. The initial and final design values are shown in Table VI. The final mapping is given by

$$\mathbf{B}^{\text{PSM}} = \begin{bmatrix} 0.570 & 0.168 & 0.209 & 0.911 & 0.214 \\ -0.029 & 0.154 & 0.126 & -0.024 & 0.470 \end{bmatrix}.$$

We notice that $[L_1 \ L_2]$, represented by the last two columns, are dominant parameters.

We run Algorithm 3 using all design parameters in the PE and in calculating the quasi-Newton step in the fine space, i.e., we use a full mapping. The algorithm converges in five iterations, however, the PE process takes 75 min on an IBM-IntelliStation¹ machine. The initial and final designs are given in Table VII. The final mapping is

$$\mathbf{B} = \begin{bmatrix} 0.532 & -0.037 & 0.026 & 0.017 & -0.006 \\ -0.051 & 0.543 & 0.022 & -0.032 & 0.026 \\ 0.415 & 0.251 & 1.024 & 0.073 & 0.011 \\ 0.169 & -0.001 & -0.022 & 0.963 & 0.008 \\ -0.213 & -0.003 & -0.045 & -0.052 & 0.958 \end{bmatrix}.$$

The reduction of $\|\mathbf{x}_c - \mathbf{x}_c^*\|_2$ versus iteration is shown in Fig. 16.

The notion of tuning is evident in this example also, where the various lengths and widths which constitute the designable parameters (see Fig. 11) have obvious physical interrelations.

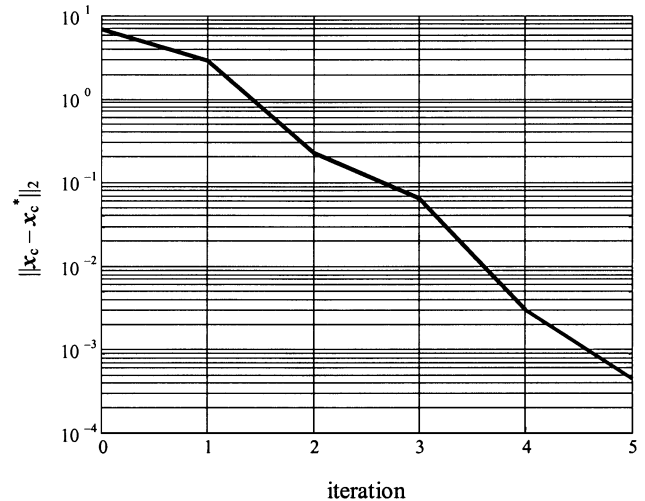


Fig. 15. $\|\mathbf{x}_c - \mathbf{x}_c^*\|_2$ versus iteration for the bandstop microstrip filter using L_1 and L_2 as the PSM coarse-model parameters.

TABLE VI
INITIAL AND FINAL DESIGNS FOR THE BANDSTOP MICROSTRIP FILTER USING L_1 AND L_2

Parameter	$\mathbf{x}_f^{(0)}$	$\mathbf{x}_f^{(5)}$
W_1	4.560	7.329
W_2	9.351	10.672
L_0	107.80	109.24
L_1	111.03	115.53
L_2	108.75	111.28

All values are in mils

TABLE VII
INITIAL AND FINAL DESIGNS FOR THE BANDSTOP MICROSTRIP FILTER USING A FULL MAPPING

Parameter	$\mathbf{x}_f^{(0)}$	$\mathbf{x}_f^{(5)}$
W_1	4.560	8.7464
W_2	9.351	19.623
L_0	107.80	97.206
L_1	111.03	116.13
L_2	108.75	113.99

All values are in mils

D. Comparison With Previous Approaches

All SM-based algorithms, by their very nature, are expected to produce acceptable designs in a small number of fine-model evaluations, typically 3–10. Hence, a basis for comparison must be simplicity, ease of programming, robustness on many examples and, in particular, avoidance of designer intervention. Our extensive convergence results (Tables I and II, Figs. 9, 10, 15, and 16) of our gradient-based proposal demonstrate that we averted false parameter extractions, do not require sophisticated programming, and do not rely on designer intervention.

¹AMD Athlon, 400 MHz.

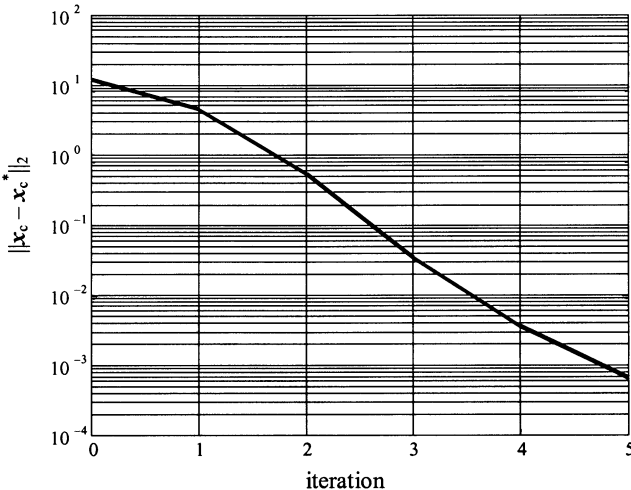


Fig. 16. $\|x_c - x_c^*\|_2$ versus iteration for the bandstop microstrip filter using a full mapping.

V. CONCLUSIONS

We present a family of robust techniques for exploiting sensitivities in EM-based circuit optimization through SM. We exploit a PSM concept where a reduced set of parameters is sufficient in the PE process. Available gradients can initialize mapping approximations. Exact or approximate Jacobians of responses can be utilized. For flexibility, we propose different possible “mapping matrices” for the PE processes and SM iterations. Finite differences may be used to initialize the mapping. A hybrid approach incorporating the Broyden formula can be used for mapping updates. Our approaches have been tested on several examples. They demonstrate simplicity of implementation, robustness, and do not rely on designer intervention.

Final mappings are useful in statistical analysis and yield optimization. Furthermore, the notion of exploiting reduced sets of physical parameters reflects the importance of the idea of post-production tuning.

ACKNOWLEDGMENT

The authors thank Dr. J.C. Rautio, President of Sonnet Software, Inc., Liverpool, NY, for making *em* available.

REFERENCES

- [1] J. W. Bandler, R. M. Biernacki, S. H. Chen, P. A. Grobelny, and R. H. Hemmers, “Space mapping technique for electromagnetic optimization,” *IEEE Trans. Microwave Theory Tech.*, vol. 42, pp. 2536–2544, 1994.
- [2] J. W. Bandler, R. M. Biernacki, S. H. Chen, R. H. Hemmers, and K. Madsen, “Electromagnetic optimization exploiting aggressive space mapping,” *IEEE Trans. Microwave Theory Tech.*, vol. 43, pp. 2874–2882, 1995.
- [3] J. Snel, “Space mapping models for RF components,” *IEEE MTT-S IMS*, 2001.
- [4] D. G. Swanson Jr and R. J. Wenzel, “Fast analysis and optimization of combline filters using FEM,” *IEEE MTT-S IMS Dig.*, pp. 1159–1162, 2001.
- [5] J. W. Bandler, W. Kellermann, and K. Madsen, “A superlinearly convergent minimax algorithm for microwave circuit design,” *IEEE Trans. Microwave Theory Tech.*, vol. MTT-33, pp. 1519–1530, 1985.

- [6] M. H. Bakr, J. W. Bandler, M. A. Ismail, J. E. Rayas-Sánchez, and Q. J. Zhang, “Neural space-mapping optimization for EM-based design,” *IEEE Trans. Microwave Theory Tech.*, vol. 48, pp. 2307–2315, 2000.
- [7] J. W. Bandler, Q. J. Zhang, and R. M. Biernacki, “A unified theory for frequency-domain simulation and sensitivity analysis of linear and nonlinear circuits,” *IEEE Trans. Microwave Theory Tech.*, vol. 36, pp. 1661–1669, 1988.
- [8] J. W. Bandler, Q. J. Zhang, J. Song, and R. M. Biernacki, “FAST gradient based yield optimization of nonlinear circuits,” *IEEE Trans. Microwave Theory Tech.*, vol. 38, pp. 1701–1710, 1990.
- [9] F. Alessandri, M. Mongiardo, and R. Sorrentino, “New efficient full wave optimization of microwave circuits by the adjoint network method,” *IEEE Microwave Guided Wave Lett.*, vol. 3, pp. 414–416, 1993.
- [10] N. K. Georgieva, S. Glavic, M. H. Bakr, and J. W. Bandler, “Feasible adjoint sensitivity technique for EM design optimization,” *IEEE Trans. Microwave Theory Tech.*, vol. 50, pp. 2751–2758, Dec. 2002.
- [11] ———, “Adjoint variable method for design sensitivity analysis with the method of moments,” in *Proc. ACES’2002*, Monterey, CA, 2002, pp. 195–201.
- [12] M. H. Bakr, J. W. Bandler, N. K. Georgieva, and K. Madsen, “A hybrid aggressive space-mapping algorithm for EM optimization,” *IEEE Trans. Microwave Theory Tech.*, vol. 47, pp. 2440–2449, 1999.
- [13] J. W. Bandler, R. M. Biernacki, and S. H. Chen, “Fully automated space mapping optimization of 3D structures,” *IEEE MTT-S IMS Dig.*, pp. 753–756, 1996.
- [14] M. H. Bakr, J. W. Bandler, and N. K. Georgieva, “An aggressive approach to parameter extraction,” *IEEE Trans. Microwave Theory Tech.*, vol. 47, pp. 2428–2439, 1999.
- [15] J. W. Bandler, M. A. Ismail, and J. E. Rayas-Sánchez, “Expanded space-mapping design framework exploiting preassigned parameters,” *IEEE MTT-S IMS Dig.*, pp. 1151–1154, 2001.
- [16] C. G. Broyden, “A class of methods for solving nonlinear simultaneous equations,” *Math. Comp.*, vol. 19, pp. 577–593, 1965.
- [17] J. W. Bandler, S. H. Chen, S. Daijavad, and K. Madsen, “Efficient optimization with integrated gradient approximations,” *IEEE Trans. Microwave Theory Tech.*, vol. 36, pp. 444–455, 1988.
- [18] M. H. Bakr, J. W. Bandler, K. Madsen, and J. Søndergaard, “Review of the space mapping approach to engineering optimization and modeling,” *Optimiz. Eng.*, vol. 1, pp. 241–276, 2000.
- [19] R. Fletcher, *Practical Methods of Optimization*, 2nd ed. New York: Wiley, 1987.
- [20] M. H. Bakr, J. W. Bandler, K. Madsen, J. E. Rayas-Sánchez, and J. Søndergaard, “Space mapping optimization of microwave circuits exploiting surrogate models,” *IEEE Trans. Microwave Theory Tech.*, vol. 48, pp. 2297–2306, 2000.
- [21] M. Pozar, *Microwave Engineering*. Amherst, MA: Wiley, 1998.
- [22] *Matlab*, Version 6.0, The MathWorks Inc., Natick, MA, 2000.
- [23] J. W. Bandler, “Computer-aided circuit optimization,” in *Modern Filter Theory and Design*, G. C. Temes and S. K. Mitra, Eds. New York: Wiley, 1973, pp. 211–271.
- [24] *em* Version 5.1a, Sonnet Software Inc., Liverpool, NY, 1997.
- [25] *OSA90/hope and Empipe* Version 4.0, Agilent EEs of EDA, Santa Rosa, CA, 1997.



John W. Bandler (S’66–M’66–SM’74–F’78) was born in Jerusalem on November 9, 1941. He studied at Imperial College of Science and Technology, London, U.K., from 1960 to 1966. He received the B.Sc. (Eng.), Ph.D., and D.Sc. (Eng.) degrees from the University of London, London, U.K., in 1963, 1967, and 1976, respectively.

In 1966, he joined Mullard Research Laboratories, Redhill, Surrey, U.K. From 1967 to 1969, he was a Post-Doctorate Fellow and Sessional Lecturer at the University of Manitoba, Winnipeg, MB, Canada. In 1969, he joined McMaster University, Hamilton, ON, Canada, where he has served as Chairman of the Department of Electrical Engineering and Dean of the Faculty of Engineering. He is currently Professor Emeritus in Electrical and Computer Engineering, and directs research in the Simulation Optimization Systems Research Laboratory. He was President of Optimization Systems Associates Inc. (OSA), which he founded in 1983, until November 20, 1997, the date of acquisition of OSA by the Hewlett-Packard Company (HP). OSA implemented a first-generation yield-driven microwave CAD capability for Raytheon

in 1985, followed by further innovations in linear and nonlinear microwave CAD technology for the Raytheon/Texas Instruments Joint Venture MIMIC Program. OSA introduced the CAE systems RoMPE in 1988, HarPE in 1989, OSA90 and OSA90/hope in 1991, Empipe in 1992, and Empipe3D and EmpipeExpress in 1996. OSA created *empath* in 1996, marketed by Sonnet Software Inc. He is currently the President of the Bandler Corporation, Dundas, ON, Canada, which he founded in 1997. He has authored or co-authored over 340 papers. He joined the Editorial Boards of the *International Journal of Numerical Modeling* in 1987, the *International Journal of Microwave and Millimeterwave Computer-Aided Engineering* in 1989, and *Optimization and Engineering* in 1998.

Dr. Bandler was an Associate Editor of the IEEE TRANSACTIONS ON MICROWAVE THEORY AND TECHNIQUES (1969–1974), and has continued serving as a member of the IEEE Microwave Theory and Techniques Society (IEEE MTT-S) Editorial Board. He is currently the co-chair of the IEEE MTT-1 Technical Committee on Computer-Aided Design. He is a Fellow of the Royal Society of Canada, the Institution of Electrical Engineers (IEE), U.K., and the Engineering Institute of Canada, a member of the Association of Professional Engineers of the Province of Ontario, Canada, and a Member of the Massachusetts Institute of Technology (MIT) Electromagnetics Academy. He received the Automatic Radio Frequency Techniques Group (ARFTG) Automated Measurements Career Award in 1994.



Ahmed S. Mohamed (S'00) was born in Cairo, Egypt, on February 20, 1973. He received the B.Sc. degree (with distinction) in electronics and communications engineering and the Master's degree in engineering mathematics, from Cairo University, Cairo, Egypt, in 1995 and 2000, respectively. He is currently working toward the Ph.D. degree at McMaster University, Hamilton, ON, Canada.

From 1995 to 2000, he was with the Department of Engineering Mathematics and Physics, Faculty of Engineering, Cairo University. In September 2000,

he joined the Department of Electrical and Computer Engineering, McMaster University. His research, carried out in the Simulation Optimization Systems Research Laboratory, includes optimization methods, computer-aided design and modeling of microwave circuits.



Mohamed H. Bakr (S'98–M'01) received the B.Sc. degree (with honors) in electronics and communications engineering in 1992 and the Master's degree in engineering mathematics in 1996, both from Cairo University, Cairo, Egypt, and the Ph.D. degree in 2000 from the Department of Electrical and Computer Engineering, McMaster University, Hamilton, ON, Canada.

During 1997, he was an intern with Optimization Systems Associates Inc., Dundas, ON, Canada. From 1998 to 2000, he was a Research Assistant with the Simulation Optimization Systems Research Laboratory, McMaster University. In November 2000, he joined the Computational Electromagnetics Research Laboratory (CERL), University of Victoria, Victoria, BC, Canada, as an Natural Sciences and Engineering Research Council of Canada Post-Doctoral Fellow. He is currently an Assistant Professor with the Department of Electrical and Computer Engineering, McMaster University. His areas of research include optimization methods, CAD and modeling of microwave circuits, neural network applications, smart analysis of microwave circuits and efficient optimization using time-/frequency-domain methods.



Kaj Madsen was born in Hjørring, Denmark, in 1943. He received the Cand.Scient. degree in mathematics from the University of Aarhus, Aarhus, Denmark, in 1968, and the Dr.Techn. degree from the Technical University of Denmark (DTU), Lyngby, Denmark, in 1986.

During the period 1968–1988, he was a Lecturer in numerical analysis, mostly with the Department for Numerical Analysis, DTU, but also with the Computer Science Department, Copenhagen University (1981–1983) and with AERE Harwell,

Didcot, U.K. (1973–1974). During the summer of 1978, he visited McMaster University, Hamilton, ON, Canada. During the 1990s, he arranged several international workshops on linear programming, parallel algorithms, and surrogate optimization. In 1993, he joined the Department of Mathematical Modeling, DTU, and was Head of that department during 1995–2000. In 2000, he took an active part in forming the new Department of Informatics and Mathematical Modeling, which includes computer science and applied mathematics. Since January 2001, he has been heading that department. His primary fields of interest include nonlinear optimization, including space-mapping techniques and global optimization, and validated computing using interval analysis.



Jacob Søndergaard was born in Denmark, in 1975. He received the Cand.Polyt. degree in 1999 from the Technical University of Denmark, Lyngby, Denmark, where he is currently working toward the Ph.D. degree in mathematical modeling in the Department of Informatics and Mathematical Modeling.

His fields of interest include numerical analysis and optimization, with particular focus on nonlinear optimization and approximation methods.